



A turn-on chemiluminescent assay for alkaline phosphatase using two-dimensional Fe-centered metal–organic frameworks as the signaling probe

Yunyu Zhang¹ · Shanshan Li¹ · Rushi Liang¹ · Meilin Li¹ · Feiqian Wang¹ · Aiping Fan¹

Received: 3 April 2023 / Accepted: 16 May 2023 / Published online: 25 May 2023
© The Author(s), under exclusive licence to The Japan Society for Analytical Chemistry 2023

Abstract

Alkaline phosphatase (ALP) is an essential enzyme involved in cell phosphorus metabolism. Developing sensitive and accurate ALP quantitative assays is significant. In this study, a turn-on chemiluminescence (CL) analysis platform for the detection of ALP activity in human serum was established based on two-dimensional (2D) Fe-centered metal–organic frameworks with 1,3,5-benzene tricarboxylic acid as ligands (denoted as 2D Fe-BTC). The 2D Fe-BTC as the signaling probe reacts with ascorbic acid forming reduced Fe-BTC which catalyzes the luminol CL reaction producing a strong CL signal. The 2D Fe-BTC-based luminol CL reaction exhibited good CL responses when the concentration of ascorbic acid was in the range of 5–500 nM. By employing magnesium ascorbyl phosphate (MAP) as the substrate which can be hydrolyzed by ALP to generate ascorbic acid, a turn-on CL assay for the detection of ALP was established. Under optimal conditions, as low as 0.00046 U L⁻¹ of ALP could be sensitively detected with a linear range of 0.001–0.1 U L⁻¹. ALP in human serum can be detected after a simple dilution process without any other pretreatment.

Keywords Chemiluminescence · Metal–organic frameworks · Luminol · Alkaline phosphatase · Ascorbic acid

Introduction

ALP is a zinc-containing glycoprotein that catalyzes the hydrolysis of phosphate monoesters at alkaline conditions. It is an important enzyme that participates in cellular phosphorus metabolism, thus has been regarded as a biomarker for the diagnosis of a series of diseases. The abnormally increased concentration level of ALP in human serum is related to liver and bone diseases [1, 2]. Also, the lowered concentration level of ALP commonly indicates malnutrition. To further understand the role of ALP, especially on the single-cellular levels, there is a high demand for developing precise and sensitive assays to quantify ALP.

In recent years, various colorimetric [3–6], fluorescent [7–11], chemiluminescent [12–14], electrochemiluminescent [15], and electrochemical [16, 17] detection systems had been established for the detection of ALP in serum, tissues,

and cell lysates. Among these methods, the CL analytical method was featured as high sensitivity, wide linear range, and simple instrument. In recent years, L-ascorbic acid 2-phosphate trisodium salt (AAP) and MAP were reported as the substrates for the CL detection of ALP activity [18, 19]. The hydrolysis of AAP or MAP by ALP produces ascorbic acid which is commonly considered as a quencher to the luminol CL reaction. Based on the quenched CL signal, several turn-off CL sensing methods were established to detect the activity of ALP. For example, Huang's group established a luminol–H₂O₂–K₂S₂O₈ CL system with long life and high-intensity emission. Based on the quenching effect of ascorbic acid on the CL signal, a CL assay for the detection of ALP was developed using AAP as the substrate [20]. Similarly, Fan's group employed MAP as the enzymatic substrate of ALP. The hydrolysis product, ascorbic acid, quenched the gold nanoclusters-catalyzed luminol–H₂O₂ CL reaction, based on which a CL assay for the detection of ALP in human serum was developed [19]. These turn-off CL sensing methods suffered from a high background which was hard to observe the signals produced from low concentrations of ALP.

✉ Aiping Fan
fanap@tju.edu.cn

¹ School of Pharmaceutical Science and Technology, Tianjin University, Tianjin 300072, People's Republic of China

Here, we would like to report a turn-on CL sensing platform based on Fe-centered MOFs for the detection of ALP activity using MAP as the substrate. MOFs are formed by connecting metal units with organic ligands through coordination bonds. As signal probes, MOFs have received special attention in ALP detection because they have multiple active sites, large specific surface areas, and designable structures [21, 22]. Such as Tan's group employed sodium tripolyphosphate as the substrate of ALP and established a photoelectrochemical assay for the detection of ALP based on controllable sensitization of Zr-MOFs (UiO-66) with Cds quantum dots [23]. Lin's group developed a fluorescent sensing platform for the detection of ALP using pyrophosphate (PPi) as the substrate the hydrolysis product of which inhibited the fluorescent signals of *o*-phenylenediamine (OPD) oxidized by $\text{NH}_2\text{-Cu-MOFs}$. In the CL analysis field, Du's group designed a label-free chemiluminescent resonance energy transfer (CRET) platform for the detection of ALP using adenosine 5'-monophosphate (5'-AMP) as the substrate and Tb@Zn-MOFs as the signaling probe. The hydrolysis of 5'-AMP by ALP produced PO_4^{3-} ions that reacted with Tb^{3+} ions to form Tb-PO_4^{3-} resulting in a low CRET efficiency and a decrease in the CL signal [24].

Metal organic framework nanosheets are a new member of ultrathin 2D nanomaterials that combine the advantages of 2D nanomaterials with MOF crystals. As a canonical type of metal organic framework nanosheet, 2D Fe-BTC was built by connecting ferric ions and benzene tricarboxylic acid linkers [6, 25, 26]. To the best of our knowledge, the employment of 2D Fe-BTC as the signaling probe for the detection of ALP has not been reported yet. In the present study, the enhancement effect of ascorbic acid on the luminol-Fe-BTC system was discovered for the first time, which provided us with a good opportunity to develop a turn-on CL assay for the detection of ALP by using MAP as the enzyme substrate. The turn-on CL assay has the advantage of low background, thus, achieving sensitive and precise detection of ALP.

Experiment

Chemicals

Polyvinylpyrrolidone (PVP), alkaline phosphatase (from calf intestinal, 2000 U mg^{-1}), α -glucosidase (from *Saccharomyces*, 33 U mg^{-1}), cysteine, and arginine were provided by Yuanye Bio-Technology Co., Ltd. (Shanghai China). MAP was purchased from Dibai Bio-Technology Co., Ltd. (Shanghai, China). H_3BTC and glutathione (GSH) were purchased from Heowns Biochemical Technology Co, Ltd. (Tianjin, China). β -D glucose was obtained from Tokyo Chemical Industry Co., Ltd. (Tokyo, Japan). Methanol,

ferric chloride hexahydrate ($\text{FeCl}_3 \cdot 6\text{H}_2\text{O}$), copper chloride dihydrate ($\text{CuCl}_2 \cdot 2\text{H}_2\text{O}$), magnesium chloride hexahydrate ($\text{MgCl}_2 \cdot 6\text{H}_2\text{O}$), Ferrous chloride tetrahydrate ($\text{FeCl}_2 \cdot 4\text{H}_2\text{O}$) and tris(hydroxymethyl)aminomethane (Tris) were obtained from Jiangtian Chemical Co., Ltd. (Tianjin, China). Luminol was purchased from Alfa Aesar. Bovine serum albumin (BSA) and uric acid were obtained from Sigma-Aldrich. L-Ascorbic acid was obtained from Kermel Chemical Reagent Co., Ltd. (Tianjin, China). Human serum was obtained from Puboxin Bio-Technology Co., Ltd. (Beijing, China). ALP activity assay kit for the determination of ALP in serum samples was purchased from Boxbio Science and Technology Co., Ltd. (Beijing, China). Ultrapure water (18.24 M Ω) purified by an ultrapure water purification system of Youpu Co., Ltd. (Sichuan, China) was used in all experiments.

The 20 \times hydrolysis buffer solution was prepared by dissolving 24.2 mg of Tris, 14.92 g of KCl, and 4 mg of Triton X-100 in 100 mL of volumetric flasks and then made up to the scale with water.

The hydrolysis buffer solution was 1 \times hydrolysis buffer containing 0.2 mg mL^{-1} of BSA and 5 mM MgCl_2 .

Apparatus

CL emission spectra were detected by a BPCL chemiluminescence analyzer purchased from Microphotonics Technologies Co., Ltd. (Guangzhou, China). The BPCL chemiluminescence analyzer was equipped with a series of high-energy optical filters of 320, 350, 380, 400, 425, 440, 460, 490, 535, 555, and 575 nm. CL intensity measurements were performed on Fluoroskan Ascent FL microplate reader (Thermo Scientific, US). Transmission electron microscopic (TEM) images were recorded on a high-resolution transmission electron microscope (FEI Tecnai G2 F20, US). Fourier transformation infrared (FT-IR) spectra were recorded on a Tensor 27 FT-IR spectrophotometer (Bruker, Germany). The X-ray photoelectron spectra (XPS) were determined on ThermoFisher Escalab 250Xi (Thermal Electron, US).

Synthesis of 2D Fe-BTC

2D Fe-BTC MOF was synthesized according to previous reports [26]. Firstly, Cu_2O was synthesized by mixing 0.0134 g CuCl_2 and 0.1 g PVP in 40 mL of water. Then, 2.5 mL of 100 mM ascorbic acid and 2.5 mL of 200 mM NaOH were added to the mixture slowly. The reaction solution was kept stirring at room temperature for 0.5 h. The product was separated by centrifugation at 10,000 rpm for 6 min and washed three times with ethanol. The Cu_2O was dispersed in 10 mL of ethanol and used to prepare Cu-BTC. To prepare Cu-BTC, 10 mL of Cu_2O was mixed with 4 mL 50 mg mL^{-1} H_3BTC and 400 mg PVP K_{30} dissolved in 60 mL of water. After stirring at room temperature

for 16 h, a blue precipitate was obtained after centrifugation at 10,000 rpm for 16 min. The blue precipitate was washed twice with ethanol and water, respectively. Then, the product was vacuum-dried overnight at 60 °C. Finally, the 2D Fe-BTC was synthesized by substituting the Cu^{2+} ions in Cu-BTC with Fe^{3+} ions. Briefly, 10 mg of Cu-BTC was dispersed in 10 mL of water and mixed with 10 mL of 3 mg mL^{-1} FeCl_3 , the mixture of which was stirred at room temperature for 3 h. The color of the reaction solution changed from blue to yellow indicating the formation of 2D Fe-BTC. The final product was obtained by centrifugation at 10,000 rpm for 10 min and washed twice with ethanol and water, respectively. The product was vacuum-dried overnight under 60 °C. The stock solution of 2D Fe-BTC was prepared by dispersing Fe-BTC ultrapure water with a concentration of 1 mg mL^{-1} .

CL detection of ascorbic acid

For the CL detection of ascorbic acid, 50 μL of different concentrations of ascorbic acid prepared in ultrapure water was mixed with 50 μL of $10 \mu\text{g mL}^{-1}$ Fe-BTC suspension in the well of a 96-well plate and incubated at room temperature for 5 min. Then, 100 μL of 2 mM luminol in 0.1 M Tris-HCl buffer solution (pH 9) was injected into the well by a dispenser. The CL intensity was monitored by the Fluoroskan Ascent FL microplate reader. Each sample was detected three times parallelly.

CL detection of ALP

For the CL detection of ALP, 20 μL of 100 μM MAP was mixed with 180 μL of ALP with different concentrations in a hydrolysis buffer and incubated at 37 °C for 60 min. 50 μL of the resultant solution was mixed with 50 μL of $10 \mu\text{g mL}^{-1}$

Fe-BTC in the well of a 96-well plate. The following steps were the same as described above.

Results and discussion

Effect of ascorbic acid on luminol-Fe-BTC CL reaction

Ascorbic acid as a broad-spectrum scavenger for oxygen-related species is commonly considered to be a quencher in the luminol CL reaction and has been employed to study the mechanism of luminol CL reactions [27]. However, an interesting phenomenon we found was that a strong CL emission was observed when the luminol solution was injected into the mixture of 2D Fe-BTC and ascorbic acid. As shown in Fig. 1a, when 100 μL of 2 mM luminol was injected into the mixture of 2D Fe-BTC ($100 \mu\text{g mL}^{-1}$) and ascorbic acid (1 μM), a flash-type CL signal was observed. The CL signal reached the maximum after 0.3 s of injecting luminol into the mixture. In contrast, when the luminol solution was injected into 100 $\mu\text{g mL}^{-1}$ Fe-BTC or 1 μM ascorbic acid respectively, very weak CL signals were produced. The result demonstrated that the 2D Fe-BTC or ascorbic acid alone had no enhancement effect in the luminol CL reaction. However, when the 2D Fe-BTC was mixed with ascorbic acid, an about 30-fold enhanced CL signal was observed. What's more, the CL intensity of the luminol CL reaction increased by prolonging the incubation time of Fe-BTC with ascorbic acid (Fig. 1b). We speculated that the incubation of Fe-BTC with ascorbic acid may generate a product catalyzing the luminol CL reaction even without any additional oxidants.

To verify our hypothesis, the UV-Vis spectra of each reactant and their mixtures were recorded first (Fig. 2a).

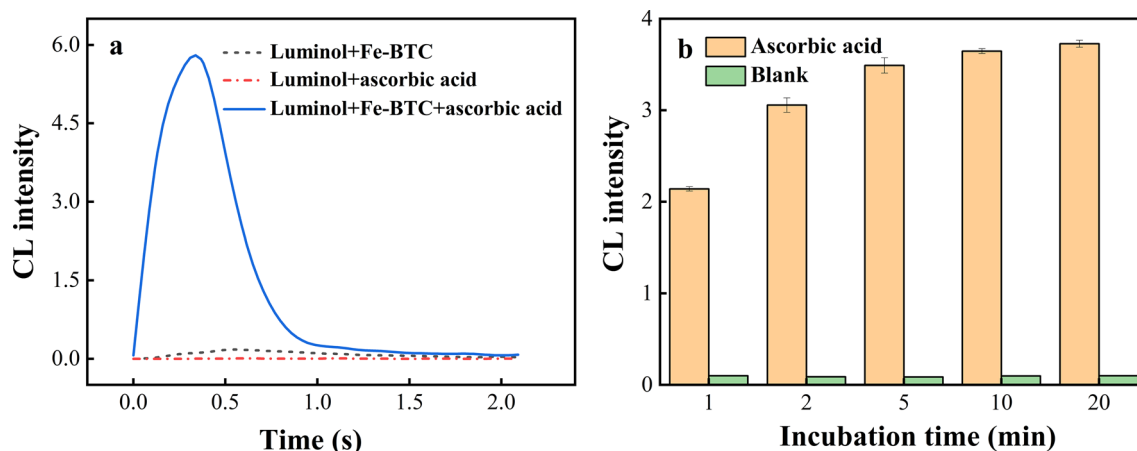


Fig. 1 **a** The CL kinetic curves and **b** the influence of incubation time on the CL reaction. Experimental conditions: 10 μM ascorbic acid, 1 mM luminol in 0.1 M Tris-HCl buffer solution (pH 10), $100 \mu\text{g mL}^{-1}$ Fe-BTC

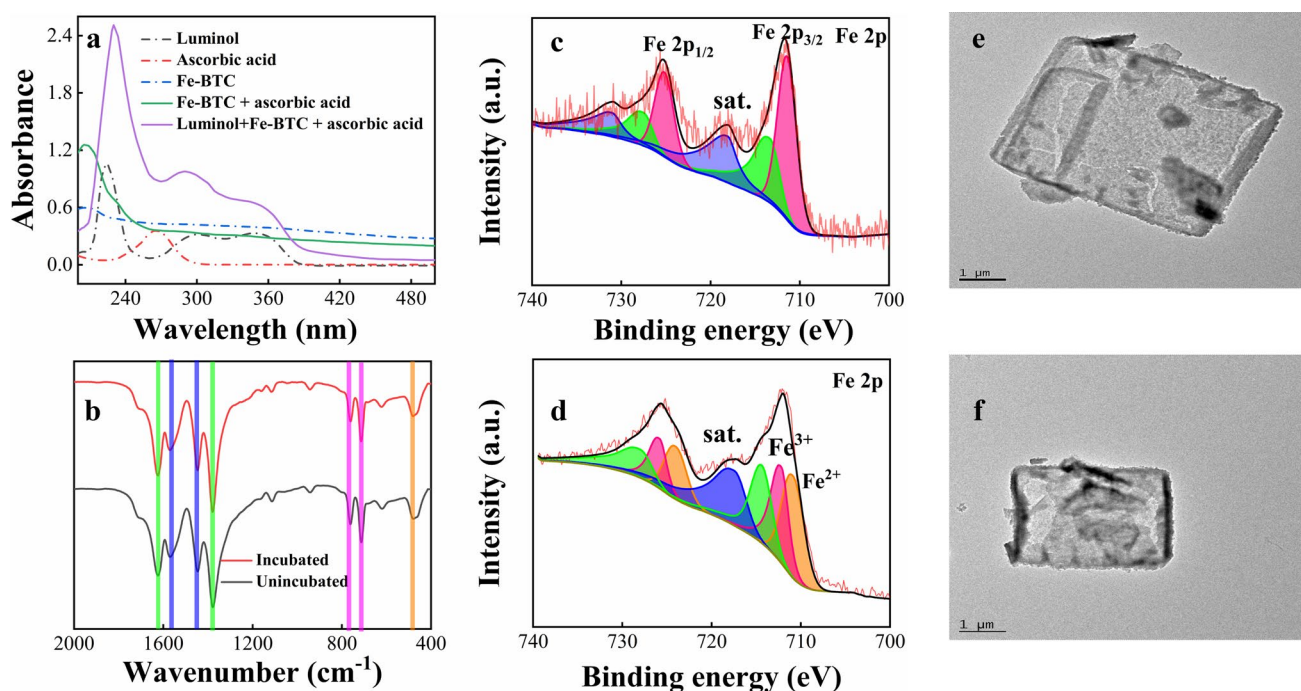


Fig. 2 **a** UV–Vis spectra of each reactant and their mixtures. **b** FT-IR spectra of 2D Fe-BTC incubated with and without ascorbic acid. **c, d** XPS spectra of Fe 2*p* peaks and **e, f** TEM images of the 2D Fe-BTC incubated without (**e, e**) or with (**d, f**) ascorbic acid

The characteristic absorption bands of luminol are located at 224 nm, 300 nm, and 345 nm, respectively. After the CL reaction, the absorption bands at 224 nm and 300 nm moved to 230 nm and 290 nm which indicated the transformation of phthalic hydrazide to phthalate ions. The maximum absorption wavelength of ascorbic acid was located at 265 nm while Fe-BTC showed terminal adsorption around 210 nm. The incubation of ascorbic acid with the 2D Fe-BTC resulted in the disappearance of the absorption peak of ascorbic acid located at 265 nm suggesting that ascorbic acid may be oxidized by the Fe-BTC. Then, the FT-IR spectra of the 2D Fe-BTC before and after the CL reaction were determined. As shown in Fig. 2b, the FT-IR spectra for both cases exhibited a similar profile. The characteristic absorption bands located at 1621 cm^{-1} , 1568 cm^{-1} , 1441 cm^{-1} , 1375 cm^{-1} , 760 cm^{-1} and 710 cm^{-1} were ascribed to benzene tricarboxylic acid in Fe-BTC. This result indicated that the ligand (BTC) didn't take part in the redox reaction with ascorbic acid. Besides, the Fe-BTC after the CL reaction also showed an absorption band at 472 cm^{-1} which was correlated with the stretching vibration of (Fe–O) in Fe-BTC suggesting that the chelating of iron ions with ligands still existed. To investigate the valent state of iron ions in Fe-BTC after the CL reaction, the XPS of the Fe-BTC before and after the CL reaction were determined. Figure 2c is the high-resolution spectra of Fe 2*p* of Fe-BTC before

the CL reaction. The Fe-BTC without incubation with ascorbic acid exhibited two characteristic peaks at 711.7 and 725.5 eV, respectively, which were attributed to Fe 2*p*_{3/2} and Fe 2*p*_{1/2}. After incubating with ascorbic acid, the Fe-BTC exhibited two broadened peaks at 711.9 and 725.7 eV. (Fig. 2d). This discrepancy was ascribed to the formation of Fe²⁺. The peaks at 711.2 and 724.2 eV were assigned to Fe²⁺. The XPS spectra suggested that the incubation of the 2D Fe-BTC with ascorbic acid resulted in the reduction of Fe³⁺ to Fe²⁺ ions. To verify the generation of Fe²⁺, 1,10-phenanthroline that reacts with Fe²⁺ to produce a coordination complex having a maximum absorption at 510 nm was employed. 100 $\mu\text{g mL}^{-1}$ of Fe-BTC was incubated with 500 μM ascorbic acid at room temperature for 20 min, to which 50 μL of 60 mg L^{-1} 1,10-phenanthroline was then added. Consistent with our hypothesis, the reaction product showed maximum absorption at 510 nm (Fig. S1). The results suggested that the incubation of Fe-BTC with ascorbic acid led to the reduction of Fe³⁺ ions in 2D Fe-BTC to Fe²⁺ ions. The reduced Fe-BTC was an efficient catalyst in the luminol CL reaction that catalyzed the oxidation of luminol to emit light even without additional oxidants. Besides, the TEM images of the 2D Fe-BTC before and after the CL reaction were determined. Before the CL reaction, the 2D Fe-BTC had a transverse size of 5 μm (Fig. 2e). After incubating with ascorbic acid, the structure of 2D Fe-BTC was still maintained (Fig. 2f).

CL mechanism studies

The CL emission spectra were determined on the BPCL analyzer equipped with a series of light filters. Figure 3 is the CL spectra of the CL reaction with and without the addition of ascorbic acid, respectively. When 2 mM luminol was injected into 100 μL of 50 $\mu\text{g mL}^{-1}$ 2D Fe-BTC directly, a weak CL emission located at 425 nm was observed. In the case of incubating the 2D Fe-BTC with 10 μM ascorbic acid, an enhanced CL emission at 425 nm was obtained.

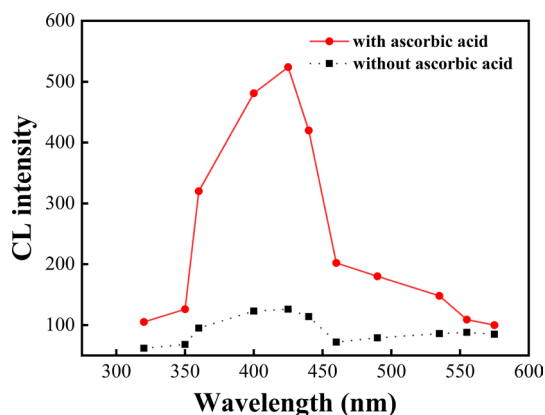
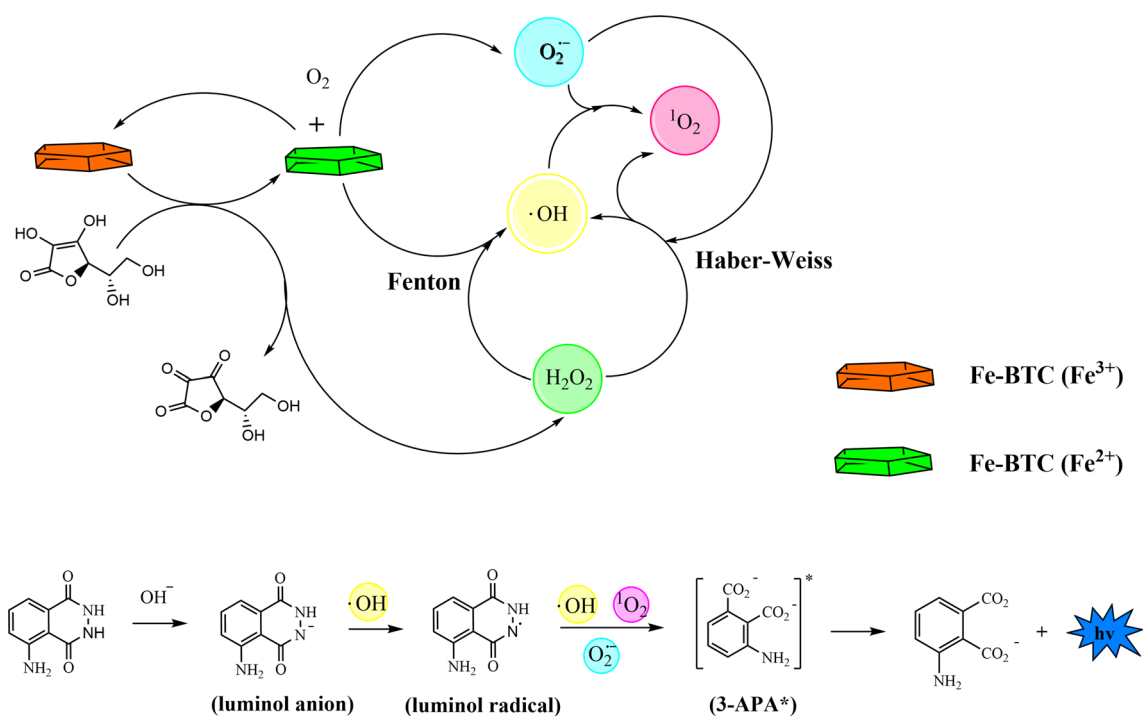


Fig. 3 CL spectra of the CL reaction with and without the addition of ascorbic acid. Experimental conditions: 2 mM luminol in 0.1 M Tris-HCl buffer solution (pH 9), 50 $\mu\text{g mL}^{-1}$ Fe-BTC

The maximum emission wavelength at 425 nm suggested the luminophores of both cases were still 3-aminophthalate anions in excited states (3-APA*).

Because there is no additional oxidant added to the CL reaction, the dissolved oxygen was considered as one of the oxidants to oxidize luminol to produce the 3-APA*. To explore the role of dissolved oxygen in the CL reaction, the CL signal was determined after bubbling all of the CL reaction solutions with gas N_2 for 30 min to remove dissolved O_2 . The CL intensity decreased by 14.6% proving that dissolved oxygen participated in the CL reaction. Besides, H_2O_2 which was produced from the redox reaction of the 2D Fe-BTC with ascorbic acid may be the other oxidant in the CL reaction [28]. Then, to explore the types of oxygen-related free radicals involving in the CL reaction, different kinds of free-radical scavengers were added to the CL solution. The CL intensity decreased by 67.3%, 57.5%, and 94.2% in the presence of 5% methanol, 10 U of superoxide dismutase (SOD), and 0.5 mM histidine, respectively. The results suggested that hydroxyl radicals ($\cdot\text{OH}$), superoxide anion radical ($\text{O}_2^{\cdot-}$), and singlet oxygen ($^1\text{O}_2$) were involved in the luminol-Fe-BTC-ascorbic acid CL reaction. The possible mechanism was summarized in Scheme 1. The 2D Fe-BTC reacted with ascorbic acid producing reduced Fe-BTC and H_2O_2 . The reduced Fe-BTC that has Fe^{2+} ions may undergo a classical Fenton reaction with H_2O_2 to generate $\cdot\text{OH}$ which oxidized luminol anions to form luminol radicals. Also, the reduced Fe-BTC may react with dissolved O_2 to form



Scheme 1 The possible mechanism of the luminol-Fe-BTC-ascorbic acid CL system

Fe-BTC and $O_2^{\cdot-}$. The Haber–Weiss reaction may occur between $O_2^{\cdot-}$ and H_2O_2 to produce $\cdot OH$ and 1O_2 . Besides, 1O_2 may also be produced from the reaction of $\cdot OH$ and $O_2^{\cdot-}$. Finally, the luminol radicals were oxidized by these oxygen-related species including $\cdot OH$, $O_2^{\cdot-}$, and 1O_2 to produce the excited-state 3-APA* that emits blue light at 425 nm.

Optimization of CL conditions

The reaction conditions including the pH of the reaction, the concentration of luminol and 2D Fe-BTC were optimized systematically by fixing the incubation time of Fe-BTC with ascorbic acid at 5 min. 0.1 M Tris–HCl buffer solution was employed to prepare the working solution of luminol and to maintain the pH of the CL reaction. As shown in Fig. 4a, a higher pH condition resulted in a stronger blank signal and a lower *S/N* ratio which referred to the signal ratio of the sample test to that of the blank test. Thus, the pH of the Tris–HCl buffer solution was set at pH 9. Figure 4b is the influence of the concentration of 2D Fe-BTC on the CL reaction. Both of sample signal and blank signal increased with higher concentrations of 2D Fe-BTC. Although the highest *S/N* ratio was obtained by using $1 \mu\text{g mL}^{-1}$ of Fe-BTC, the CL intensity at this data point was relatively low. Thus, $10 \mu\text{g mL}^{-1}$ of Fe-BTC was selected for the following studies. A higher concentration of luminol is a benefit to the CL reaction. The CL intensity of sample tests increased dramatically with an increased concentration of luminol without a significant enhancement on the blank signals (Fig. 4c). The *S/N* ratio increased linearly with the increased concentration of luminol ranging from 0.2 to 3 mM. Considering the reagent consumption, 2 mM luminol was employed in the following studies. In summary, experimental conditions including Tris–HCl buffer with pH 9, 2 mM luminol, $10 \mu\text{g mL}^{-1}$ of Fe-BTC, and 5 min of incubation time were employed in the following studies.

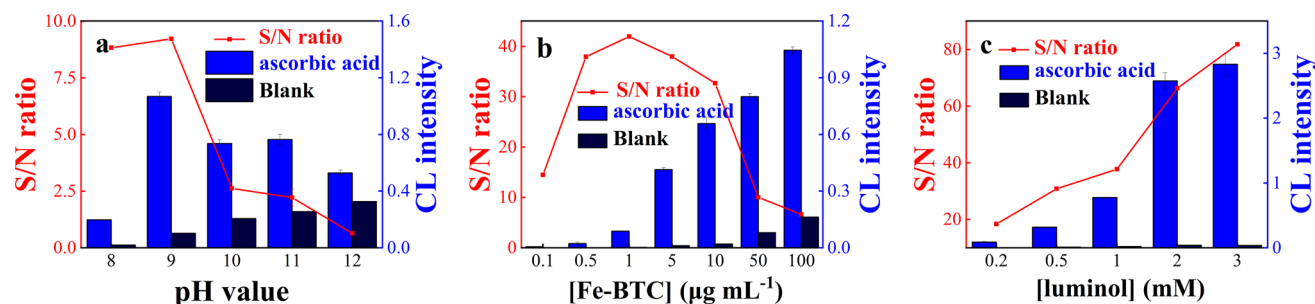


Fig. 4 Optimization of experimental conditions including **a** pH of the buffer solution, the concentration of **b** Fe-BTC, and **c** luminol. Experimental conditions: **a** $1 \mu\text{M}$ ascorbic acid, 1 mM luminol in 0.1 M Tris–HCl buffer solution with different pH values, $100 \mu\text{g mL}^{-1}$ Fe-

CL responses for ascorbic acid

To test the CL response of the luminol CL reaction to different concentrations of ascorbic acid, different concentrations of ascorbic acid were prepared in ultrapure water and mixed with $10 \mu\text{g mL}^{-1}$ Fe-BTC, respectively. After the injection of luminol solution into the mixture, the CL intensity was determined. As shown in Fig. 5, as the concentration of ascorbic acid increased from 5 to 500 nM, the CL intensity increased linearly with increasing concentration of ascorbic acid. The regression equation was described as $I = 0.00572C + 0.05943$ ($R^2 = 0.9936$). The limit of detection (LOD) for ascorbic acid was calculated to be 0.5 nM (3 δ/s). To test the repeatability of the CL reaction, two concentrations of ascorbic acid (100 and 10 nM) were determined six times under the optimized CL conditions, and the relative standard deviation (RSD) for 100 and 10 nM ascorbic acid was 0.72% and 2.83%, respectively.

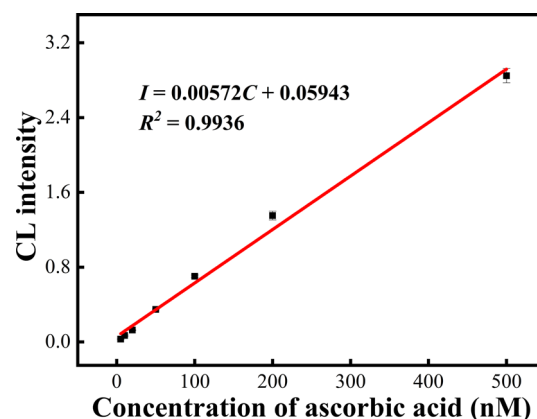


Fig. 5 Response curve of the luminol-Fe-BTC system with different concentrations of ascorbic acid

BTC. **b** pH 9 of 0.1 M Tris–HCl buffer solution, other experimental conditions were the same as (a). **c** $10 \mu\text{g mL}^{-1}$ Fe-BTC, other experimental conditions were the same as (b)

Principle of CL detection of ALP

In light of the high sensitivity of the luminol-Fe-BTC CL system for the detection of ascorbic acid, the proposed CL reaction was then applied to the detection of ALP using MAP as the substrate. MAP is phosphorylated ascorbic acid, which is more stable than ascorbic acid even after treatment at a high temperature [29]. MAP can be hydrolyzed by ALP to produce ascorbic acid and magnesium phosphate under an alkaline condition. The detection principle as shown in Scheme 2, the produced ascorbic acid then reacts with 2D Fe-BTC producing reduced Fe-BTC which catalyzes the luminol CL reaction. With the concentration of ALP increased, increasing concentrations of ascorbic acid are produced resulting in higher CL signals, thus, achieving the quantitative detection of ALP.

To verify the feasibility of the method, the CL responses of the luminol CL reaction to different concentrations of ascorbic acid in hydrolysis buffer were determined firstly. Here, different concentrations of ascorbic acid were prepared with the hydrolysis buffer solution (pH 8.5) instead of ultrapure water. The results were shown in Fig. S2 (Supporting Information). Although the CL signals of the luminol CL reaction produced by ascorbic acid in the alkaline hydrolysis buffer were lower than that prepared in ultrapure water, the CL intensity increased linearly with increasing concentration of ascorbic acid. The detection linear range

was from 20 to 500 nM, and the LOD was calculated to be 13.7 nM ($3 \delta/s$). The regression equation was described as $I = 0.0009C + 0.0435$ ($R^2 = 0.9829$). Besides, the CL signals of the luminol-Fe-BTC CL system in the presence of ALP, MAP, and both of them were determined. As shown in Fig. 6, when 100 μM MAP was incubated with 0.5 U L^{-1} ALP and then 10 $\mu\text{g mL}^{-1}$ Fe-BTC, after injecting 2 mM luminol into the reaction solution, a strong CL signal was

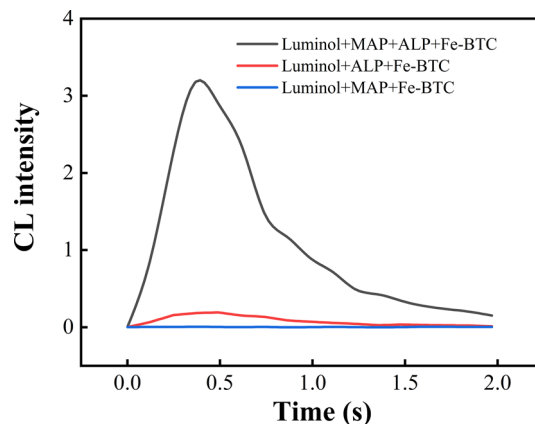
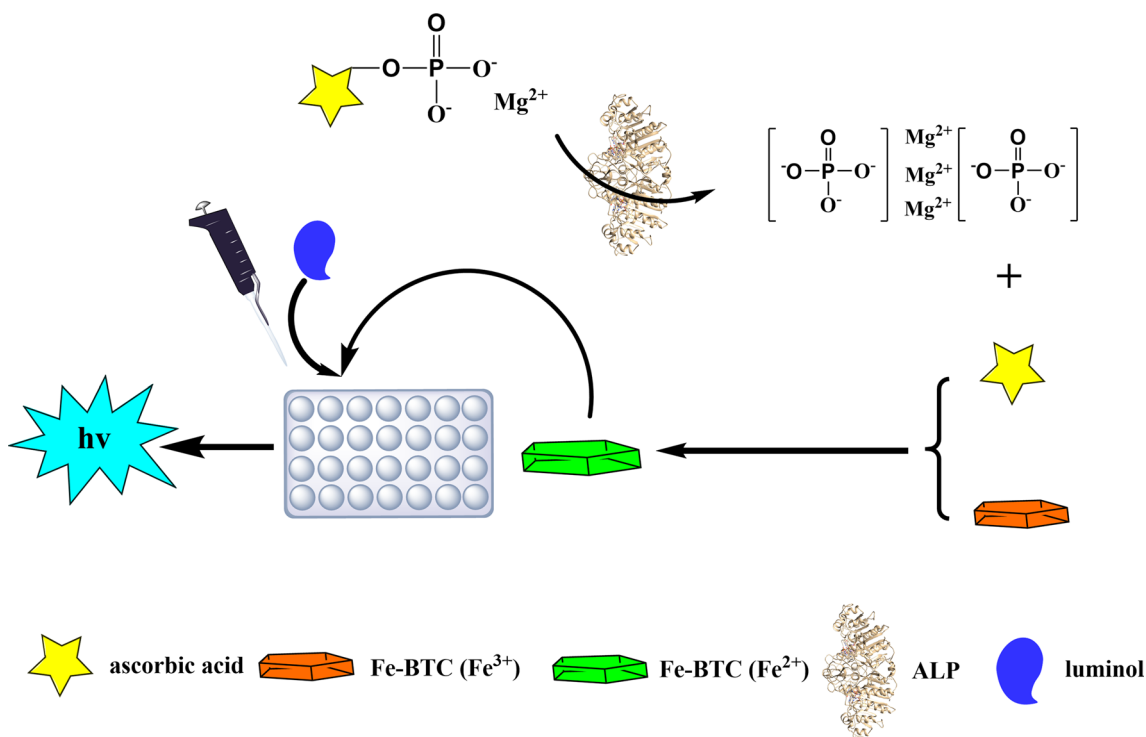


Fig. 6 The CL kinetic curves of the luminol-Fe-BTC CL system with the addition of MAP, ALP, and both of them. Experimental conditions: 100 μM MAP, 0.5 U L^{-1} ALP, 2 mM luminol in 0.1 M Tris-HCl buffer solution (pH 9), 10 $\mu\text{g mL}^{-1}$ Fe-BTC



Scheme 2 Schematic diagram of the turn-on CL assay for the detection of ALP

observed. However, if MAP or ALP alone was incubated with the 2D Fe-BTC, very weak CL signals were obtained. The results demonstrated that MAP could be employed as the substrate for the development of a turn-on CL assay for ALP by coupling the enzymatic reaction with the luminol-Fe-BTC CL reaction.

CL detection of ALP

To establish the CL assay for ALP, the influence of experimental conditions such as the concentration of MAP and incubation time of MAP with ALP on the CL detection of ALP were explored (Fig. S3, Supporting Information). When the concentration of MAP was 100 μM and the incubation time was 60 min, the S/N ratio was the highest. To evaluate the capability of the CL method for the quantitative detection of ALP, increasing concentrations of ALP were incubated with 100 μM MAP at 37 $^{\circ}\text{C}$ for 60 min and then mixed with 10 $\mu\text{g mL}^{-1}$ Fe-BTC. After injecting the

working solution of luminol into the mixture, the CL intensity was determined. As shown in Fig. 7a, the CL intensity increased linearly with the concentration of ALP in the range of 0.001–0.1 U L^{-1} . The standard curve for CL detection of ALP was described as $I = 5.0589C + 0.0159$ ($R^2 = 0.9955$). The LOD for ALP was 0.00046 U L^{-1} . Compared with previously reported methods, the proposed CL assay showed good sensitivity as well as a wide linear range (Table 1). 0.1 U L^{-1} ALP was determined 6 times and the RSD was 3.9% indicating the good repeatability of the ascorbic acid-enhanced luminol-Fe-BTC CL system for the detection of ALP. The proposed CL assay for the detection of ALP is based on the hydrolysis of MAP to produce ascorbic acid which has an enhancement effect in the luminol-Fe-BTC CL reaction. Thus, as shown in Fig. 7b, the CL system had no response to other substances including metal ions (such as Na^+ , Cu^{2+} , and Mn^{2+}), amino acids (such as Arg), and other kinds of enzymes (such as α -glucosidase), proteins (such as streptavidin and IgG) and reducing substances (such as

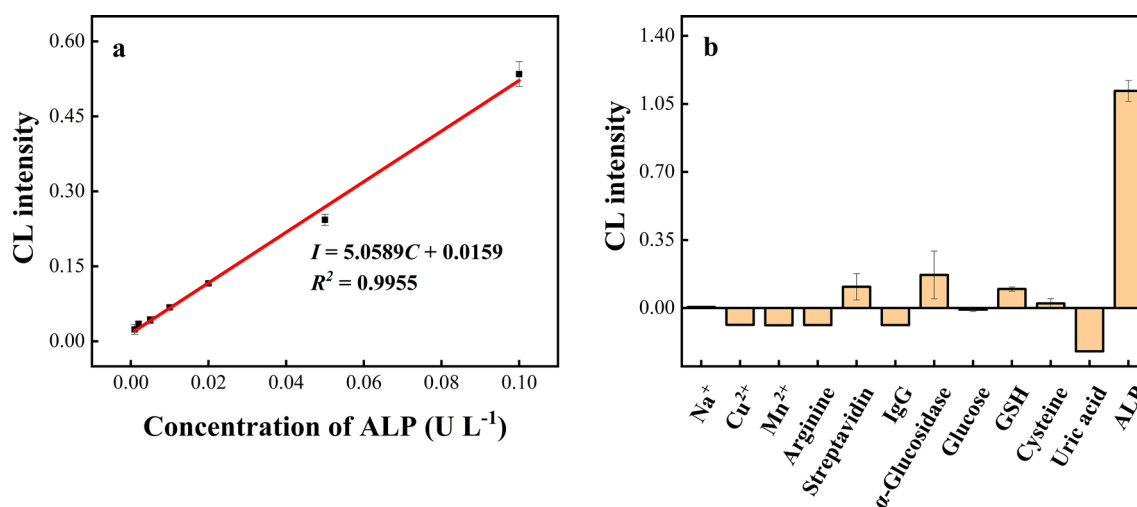


Fig. 7 a Standard curve for the CL detection of ALP. b The specificity of the luminol-Fe-BTC-MAP for the ALP detection. Experimental conditions were the same as in Fig. 6

Table 1 Comparison of our method with other ALP detection methods

Method	Material	Linear range (U L^{-1})	LOD (U L^{-1})	References
Colorimetric	His@AuNCs/graphene oxide hybrids	0–40	0.26	[4]
Fluorescent	NH_2 -Cu-MOFs	2–180	0.078	[31]
Fluorescent	ZnSe@ZnS quantum dots	4–96	0.57	[10]
Fluorescent	Fluorophore monomer P-TPE-TG	0–50	0.034	[9]
Electrochemical	Gold nanoparticle-decorated single-walled carbon nanotube	3–50	0.2	[32]
Chemiluminescent	Gold nanoclusters	0.0027–1.389	0.0026	[19]
Chemiluminescent	Fe-BTC	0.001–0.1	0.00046	This work

GSH, cysteine, glucose, and uric acid). The good selectivity was attributed to the specific hydrolysis ability of ALP to MAP which produced ascorbic acid and the specific CL response of the luminol-Fe-BTC system to ascorbic acid.

Detection of ALP in serum samples

Serum samples contain lots of substances that may affect the CL detection of ALP. To evaluate the matrix effect of serum samples on the CL detection of ALP. A commercially available serum sample was employed and pretreated at 75 °C for 10 min to inactivate ALP in the serum. Then, the deactivated serum samples were diluted at different times with the hydrolysis buffer solution and then spiked with 0.01 U L⁻¹ ALP. The CL signals were determined under optimal conditions. The results were shown in Fig. S4 (Supporting Information), the CL intensities of ALP in 100, 500, 1000, and 2000-fold diluted serum samples were significantly decreased compared with the CL signal of ALP in hydrolysis buffer solution. We assumed that the proteins in the serum may combine with the metal ions of Fe-BTC, thus preventing the reduction of Fe³⁺ by ascorbic acid. When the serum was diluted 5000 times, 0.01 U L⁻¹ ALP produced a CL signal that is similar to that produced in the hydrolysis buffer solution. Considering the concentration of ALP in normal human serum is from 70 to 90 U L⁻¹ [30], theoretically, the content of ALP in 5000-fold diluted serum sample ranges from 0.014 to 0.018 U L⁻¹ which is within the detection linear range of the proposed CL assay. Thus, the 5000-fold diluted serum sample was selected and a standard addition method was employed to evaluate the accuracy of the proposed CL method for the detection of ALP in serum samples. Three concentrations of ALP (50, 100, and 150 U L⁻¹) were spiked into the ALP-deactivated human serum samples and then diluted 5000-fold with hydrolysis buffer. The diluted samples were detected under optimal conditions. The recoveries of 50, 100, and 150 U L⁻¹ ALP were 93.3%, 100.0%, and 110.0% with RSD ranging from 2.09% to 10.1%, respectively (Table 2). Furthermore, the proposed CL method was also employed for the detection of ALP in real serum samples, the results of which were compared with results obtained from a commercial kit. The concentration of ALP in three serum samples was determined to be 23.2,

18.9, and 23.4 U L⁻¹ by using the commercial kit, while by using the proposed CL method it was determined to be 21.1, 19.4, and 23.9 U L⁻¹, respectively (Table S2, Supporting Information). The above results demonstrated the applicability of the proposed CL system for the detection of ALP in serum samples.

Conclusion

In summary, the Fe-BTC after incubating with ascorbic acid was found to enhance the luminol CL reaction. Mechanism studies showed that the incubation of Fe-BTC with ascorbic acid led to the reduction of Fe³⁺ ions in the 2D Fe-BTC to Fe²⁺ producing reduced Fe-BTC which acted as the catalyst in the luminol CL reaction. Under optimal conditions, the CL intensity increased linearly with increasing concentrations of ascorbic acid ranging from 5 to 500 nM. Based on the good CL responses of ascorbic acid in the 2D Fe-BTC-luminol CL reaction, a turn-on CL assay for the detection of ALP activity was established using MAP as the substrate. Inherent from the specific hydrolysis of the MAP by ALP to produce ascorbic acid and its specific enhancement effect on the luminol-Fe BTC CL reaction, the proposed turn-on CL assay featured good selectivity and low background. As low as 0.00046 U L⁻¹ of ALP could be sensitively detected. Benefiting from the high detection sensitivity, ALP in serum samples can be detected after a simple dilution process without any other complex pretreatments. We believed that the proposed CL assay has great potential in being applied in biochemistry, pharmaceutical analysis, and clinical diagnosis.

Supplementary Information The online version contains supplementary material available at <https://doi.org/10.1007/s44211-023-00370-0>.

Acknowledgements This research was supported by the National Natural Science Foundation of China (21475094).

Data availability The datasets generated during and/or analysed during the current study are available from the corresponding author on reasonable request.

Declarations

Conflict of interest We declare that we do not have any commercial or associative interest that represents a conflict of interest in connection with the work submitted.

References

1. X. Liu, X. Xing, B. Li, Y. Guo, Y. Zhang, Y. Yang, L. Zhang, *Biosens. Bioelectron.* **81**, 460–464 (2016). <https://doi.org/10.1016/j.bios.2016.03.030>
2. H. Zhang, L. Zhang, J. Jiang, R. Yu, *Anal. Sci.* **29**, 193–198 (2013). <https://doi.org/10.2116/analsci.29.193>

Table 2 The recovery of CL detection of ALP spiked in human serum

Sample	Amount added (U L ⁻¹)	Amount found (U L ⁻¹)		Recovery (%)
		In diluted serum	In original serum	
1	150	0.028 ± 0.0006	140 ± 3.07	93.3 ± 2.05
2	100	0.020 ± 0.0009	100 ± 4.87	100.0 ± 4.87
3	50	0.011 ± 0.0010	55 ± 1.65	110.0 ± 3.29

3. A. Hayat, G. Bulbul, S. Andresescu, *Biosens. Bioelectron.* **56**, 334–339 (2014). <https://doi.org/10.1016/j.bios.2014.01.003>
4. F. Xiao, Y. Yu, Y. Wu, L. Tian, G. Zhao, H. Pang, J. Du, *Biosensors* **11**, 174 (2021). <https://doi.org/10.3390/bios11060174>
5. X. Zhou, M. Wang, M. Wang, X. Su, *A.C.S. Appl. Nano Mater.* **4**, 7888–7896 (2021). <https://doi.org/10.1021/acsnm.1c01220>
6. H. Wan, Y. Wang, J. Chen, H.-M. Meng, Z. Li, *Microchim. Acta* **188**, 1–8 (2021). <https://doi.org/10.1007/s00604-021-04785-2>
7. R. Oishi, T. Mizuta, K. Sueyoshi, T. Endo, H. Hisamoto, *Anal. Sci.* **36**, 143–145 (2020). <https://doi.org/10.2116/analsci.19C013>
8. W. Zhu, Z. Li, L. Dai, W. Yang, Y. Li, *Anal. Sci.* **39**, 297–302 (2023). <https://doi.org/10.1007/s44211-022-00241-0>
9. J. Lee, S. Kim, T.H. Kim, S.H. Lee, *RSC Adv.* **10**, 26888–26894 (2020). <https://doi.org/10.1039/D0RA03584J>
10. P. Hu, R. Huang, Y. Xu, T. Li, J. Yin, Y. Yang, Y. Liang, X. Mao, L. Ding, C. Shu, *RSC Adv.* **13**, 2311–2317 (2023). <https://doi.org/10.1039/D2RA06956C>
11. W. Kang, Y. Ding, H. Zhou, Q. Liao, X. Yang, Y. Yang, J. Jiang, M. Yang, *Microchim. Acta* **182**, 1161–1167 (2015). <https://doi.org/10.1007/s00604-014-1439-7>
12. Q. Zhang, C. Zhang, M. Yang, D. Yu, C. Yu, *Luminescence* **32**, 1150–1156 (2017). <https://doi.org/10.1002/bio.3302>
13. R. Sarver, C. Higbee, P. Biswas, L. Zhang, N. Banner, J. Rice, M. Mozola, Z. Tollakson, L. Hardrath, M. Bulthaus, J. Zangl, *Food Prot.* **82**, 2119–2125 (2019). <https://doi.org/10.4315/0362-028X.JFP-19-153>
14. S. Albillos, R. Reddy, R. Salter, *Food Prot.* **74**, 1144–1154 (2011). <https://doi.org/10.4315/0362-028X.JFP-10-422>
15. H. Wang, F. Wang, T. Wu, Y. Liu, *Anal. Chem.* **93**, 15794–15801 (2021). <https://doi.org/10.1021/acs.analchem.1c04130>
16. M. Díaz-González, C. Fernández-Sánchez, A. Costa-García, *Anal. Sci.* **18**, 1209–1213 (2002). <https://doi.org/10.2116/analsci.18.1209>
17. K. Hirakawa, M. Katayama, N. Soh, K. Nakano, T. Imato, *Anal. Sci.* **22**, 81–86 (2006). <https://doi.org/10.2116/analsci.22.81>
18. L. Cui, C. Zhu, J. Hu, X. Meng, M. Jiang, W. Gao, X. Wang, C. Zhang, *Sens. Actuators B Chem.* **374**, 132779 (2023). <https://doi.org/10.1016/j.snb.2022.132779>
19. Y. Li, R. Wang, A. Fan, *Anal. Sci.* **36**, 1075–1079 (2020). <https://doi.org/10.2116/analsci.20P098>
20. X. Wu, C. Yang, Z. Jiang, S. Xiao, X. Wang, C. Hu, S. Zhen, D. Wang, C. Huang, Y. Li, *Microchim. Acta.* **189**, 1–8 (2022). <https://doi.org/10.1007/s00604-022-05287-5>
21. J. Xu, H. Zhang, W. Zhang, P. Li, W. Zhang, H. Wang, B. Tang, *Chem. Commun.* **56**, 2431–2434 (2020). <https://doi.org/10.1039/C9CC08828H>
22. L. Xiong, L. Yu, S. Li, L. Feng, Y. Xiao, *Microchim. Acta.* **188**, 236 (2021). <https://doi.org/10.1007/s00604-021-04880-4>
23. Y. Ying, W. Wu, G. He, W. Deng, Y. Tan, Q. Xie, *Chem. Commun.* **58**, 7960–7963 (2022). <https://doi.org/10.1039/D2CC02302D>
24. H. Li, Y. Sun, Y. Li, J. Du, *Microchem. J.* **160**, 105665 (2021). <https://doi.org/10.1016/j.microc.2020.105665>
25. J. Bao, J. Mei, X. Cheng, D. Ren, G. Xu, F. Wei, Y. Sun, Q. Hu, Y. Cen, *Microchim. Acta.* **188**, 3 (2021). <https://doi.org/10.1007/s00604-021-04701-8>
26. A. Yuan, Y. Lu, X. Zhang, Q. Chen, Y. Huang, *J. Mater. Chem. B.* **8**, 9295–9303 (2020). <https://doi.org/10.1039/D0TB01598A>
27. X. Yi, W. Dong, X. Zhang, J. Xie, Y. Huang, *Anal. Bioanal. Chem.* **408**, 8805–8812 (2016). <https://doi.org/10.1007/s00216-016-9681-y>
28. G. Buettner, T. Doherty, T. Bannister, *Radiat. Environ. Biophys.* **23**, 235–243 (1984). <https://doi.org/10.1007/BF01407595>
29. S. Kandil, I. Soliman, H. Diab, N. Bedair, M. Mahrous, E. Abdou, *Drug Deliv.* **29**, 534–547 (2022). <https://doi.org/10.1080/10717544.2022.2036872>
30. C. Rhee, M. Molnar, W. Lau, V. Ravel, C. Kovesdy, R. Mehrotra, K. Kalantar-Zadeh, *Perit. Dial. Int. J. Int. Soc. Perit. Dial.* **34**, 732–748 (2014). <https://doi.org/10.3747/pdi.2013.00110>
31. L. Hou, Y. Qin, J. Li, S. Qin, Y. Huang, T. Lin, L. Guo, F. Ye, S. Zhao, *Biosens. Bioelectron.* **143**, 111605 (2019). <https://doi.org/10.1016/j.bios.2019.111605>
32. L. Zhao, L. Zhao, Y. Miao, C. Zhang, *Int. J. Electrochem. Sci.* **13**, 1293–1307 (2018). <https://doi.org/10.20964/2018.02.04>

Springer Nature or its licensor (e.g. a society or other partner) holds exclusive rights to this article under a publishing agreement with the author(s) or other rightsholder(s); author self-archiving of the accepted manuscript version of this article is solely governed by the terms of such publishing agreement and applicable law.